8-2009

Minimum Transmission Power Configuration in Real-Time Wireless Sensor Networks

Xiaodong Wang
University of Tennessee - Knoxville

To the Graduate Council:

I am submitting herewith a thesis written by Xiaodong Wang entitled "Minimum Transmission Power Configuration in Real-Time Wireless Sensor Networks." I have examined the final electronic copy of this thesis for form and content and recommend that it be accepted in partial fulfillment of the requirements for the degree of Master of Science, with a major in Computer Engineering.

Xiaorui Wang, Major Professor

We have read this thesis and recommend its acceptance:

Gregory D. Peterson, Husheng Li

Accepted for the Council:
Dixie L. Thompson

Vice Provost and Dean of the Graduate School

(Original signatures are on file with official student records.)

To the Graduate Council:

I am submitting herewith a thesis written by Xiaodong Wang entitled "Minimum Transmission Power Configuration in Real-Time Wireless Sensor Networks". I have examined the final electronic copy of this thesis for form and content and recommend that it be accepted in partial fulfillment of the requirements for the degree of Master of Science with a major in Computer Engineering.

Xiaorui Wang, Major Professor

We have read this thesis
and recommend its acceptance:

Gregory D. Peterson

Husheng Li

Accepted for the Council:

Carolyn R. Hodges,

Vice Provost and Dean of the Graduate School

(Original signatures are on file with official student records)

Minimum Transmission Power Configuration in Real-Time Wireless Sensor Networks

A Thesis Presented for
the Master of Science Degree
The University of Tennessee, Knoxville

Xiaodong Wang
August 2009

Acknowledgements

First and foremost, I would like to thank my advisor Dr. Xiaorui Wang for the motivation and guidance, without which this work would not have been possible. I would also like to thank Dr. Gregory D. Peterson and Dr. Husheng Li for serving on my committee. Moreover, I would like to thank Dr. Guoliang Xing at Michigan State University for his valuable support and suggestions on this thesis.

Abstract

Multi-channel communications can effectively reduce channel competition and interferences in a wireless sensor network, and thus achieve increased throughput and improved end-to-end delay guarantees with reduced power consumption. However, existing work relies only on a small number of orthogonal channels, resulting in degraded performance when a large number of data flows need to be transmitted on different channels. In this thesis, empirical studies are conducted to investigate the interferences among overlapping channels. The results show that overlapping channels can also be utilized for improved real-time performance if the node transmission power is carefully configured. In order to minimize the overall power consumption of a network with multiple data flows under end-to-end delay constraints, a constrained optimization problem is formulated to configure the transmission power level for every node and assign overlapping channels to different data flows. Since the optimization problem has an exponential computational complexity, a heuristic algorithm designed based on Simulated Annealing is then presented to find a suboptimal solution. The extensive empirical results on a 25-mote testbed demonstrate that the proposed algorithm achieves better real-time performance and less power consumption than two baselines including a scheme using only orthogonal channels.

Table of Contents

List of Tables

List of Figures

Chapter 1 Introduction

1.1 Current Multi-channel Real-time Wireless Sensor Networks

Many wireless sensor network (WSN) applications must address multiple stringent design constraints such as energy consumption and end-to-end communication delay. Energy has long been treated as the primary optimization goal for battery-powered wireless sensor nodes. With lower energy consumption, a network can achieve a longer lifetime. In addition to periodic sleeping, one of the effective ways to reduce node energy consumption is to lower its radio transmission power. This can be supported by the existing sensor mote hardware. For example, the CC2420 radio chip [1] used in many mote hardware platforms has 31 different transmission power levels. However, reduced transmission power may lead to unreliable wireless links and cause increased number of retransmissions. As a result, it may lead to poor guarantees of other important design constraints such as end-to-end delay, as many WSN applications require information to be transmitted from sources to sinks within an application-specified deadline. Therefore, transmission power must be carefully configured in order to meet the desired constraints of a WSN. High transmission power may improve the quality of a single wireless link but may lead to increased power consumption, stronger interferences to other links, and reduced network capacity [2].

The emergence of multi-channel mote hardware has made it possible to achieve improved throughput and delay guarantees with reduced transmission power, by greatly reducing channel competition and interferences among different nodes. As a result, multi-channel communication protocols have been proposed for WSNs to improve the performance of traditional single-channel protocols commonly used in WSNs. For example, a multi-channel protocol has been designed in [3] to improve network throughput and reduce packet loss for WSNs. Multi-channel MAC protocols [4][5] have also been proposed to improve network throughput for WSNs. Recently, a multi-channel real-time communication protocol has also been presented to allow different data flows to transmit on different channels for improved end-to-end real-time guarantees with reduced power consumption [6]. Multi-channel communications are promising because many radio chips used in today's sensor mote hardware can work at multiple frequencies. For example, the CC2420 radio chip provides 16 wireless channels with radio frequency from 2,400 to 2,483MHz.

While multi-channel communications have shown great promise, recent studies (*e.g.*, [3]) conducted experiments on Micaz hardware to investigate multi-channel realities in wireless sensor networks. An important reality reported is that the number of orthogonal channels on the existing mote hardware is actually limited. Accordingly, it has been suggested that a practical multi-channel communication protocol should only rely on a small number of non-adjacent orthogonal channels, because adjacent overlapping channels may have undesired inter-channel interferences. For example, at most, only 8 channels out of the 16 channels provided by the CC2420 radio chip can be used as orthogonal channels [3], which results in the waste of half of the available wireless

channel resources. While 8 channels may be enough for some WSN applications, using only orthogonal channels has limited the further improvement of network throughput, real-time performance, and power optimization in the commonly used many-to-one traffic pattern, where the number of data flows can be large in a network.

1.2 Contributions

This thesis work proposes to utilize adjacent overlapping channels to configure power and channels for a WSN to achieve improved real-time performance and reduced power consumption. The power and channel configuration problem is defined as follows: Given a WSN with multiple data flows from different sources to the base station, the goal is to assign channels (including overlapping channels) to the data flows and determine a transmission power level for every node in the network, such that the overall (transmission) power consumption of the network can be minimized while the average end-to-end delay of each data flow can be guaranteed to stay within a deadline. Hardware experiments are first conducted to investigate the interferences among overlapping channels as to motivate the work. Empirical studies are performed afterwards for overlapping channel modeling. Based on the models established from the empirical studies, a power and channel configuration problem as a constrained optimization problem is formulated, with power minimization as the objective and the end-to-end delay as the constraints. Since it is cost-prohibitive to find the optimal solution, a heuristic algorithm based on Simulated Annealing is proposed to find a suboptimal

solution. Finally, extensive experiments are conducted on a 25-mote testbed to show that the configuration method proposed here outperforms two baseline solutions.

More specifically, the contributions of this thesis are four-fold:

- Empirical studies are conducted to investigate the interferences among overlapping channels. The results show that overlapping channels can also be utilized for improved real-time performance if the node transmission power is carefully configured.
- Existing work is extended to establish an empirical model between received signal strength (RSS) and transmission power level for overlapping channels. Based on the RSS model, a packet reception ratio (PRR) model is derived to account for the interferences from overlapping channels.
- A power and channel configuration problem is formulated as a constrained optimization problem. Since the problem has an exponential computational complexity, a heuristic algorithm designed based on Simulated Annealing (SA) is proposed to find a suboptimal solution.
- The algorithm is implemented on the Tmote Invent hardware and extensive experiments are conducted on a 25-mote testbed. The results demonstrate that the algorithm proposed in this work can reduce both the end-to-end communication delay and overall power consumption, compared with two baselines. The first baseline conducts the same optimization using only orthogonal channels. The second baseline uses SA to find the desired power level but randomly assigns overlapping channels.

1.3 Thesis Outline

Chapter 1 was aimed on introducing the current multi-channel real-time wireless sensor networks. It also outlined the contribution of this thesis. The rest of thesis is organized as follows. Chapter 2 highlights the distinction of this work by discussing the related work. Chapter 3 presents empirical studies to motivate this work and builds models for overlapping channels. Chapter 4 introduces the formulation of a transmission power optimization problem with real-time performance analysis and presents the algorithm used in solving the optimization problem. Chapter 5 presents the empirical results of the proposed algorithm. Chapter 6 concludes the thesis.

Chapter 2 A Review of the Related Work

2.1 Overlapping Channel Utilization

Recent studies have proposed to use partially overlapping channels (POC) in wireless mesh networks. Liu et al. [7] propose a channel allocation scheme for link scheduling, which takes advantages of POC to obtain better throughput for mesh networks. Feng et al. [8] establish an interference model for POC-based wireless networks, and use numeric methods to improve overall network capacity. A linear model for channel assignment, which uses a channel overlapping matrix and mutual interference matrices to model POC channels, has been proposed in [9]. However, no detailed study has been performed for utilizing overlapping channels in wireless sensor networks. A coarse-grained channel assignment policy for WSNs is proposed in [3], which allocates non-overlapping channels to disjoint trees and exploits parallel transmissions among trees. This work proposes to utilize overlapping channels to configure power and channels for a WSN to achieve better real-time performance and energy efficiency.

2.2 Power Management

Power management, as a critical issue in wireless sensor networks, has been extensively studied. Previous work on transmission power control can be approximately classified into two categories: topology control and power-aware routing. Topology control reduces transmission power to the maximum degree for preserving the desirable

property of a wireless network (*e.g.*, connectivity). A survey on existing topology control schemes can be found in [10] and several representative projects are [11][12][13][14]. The goal of power-aware routing is to find energy-efficient routes by varying transmission power, as presented in [15][16][17][18][19]. Although the above studies demonstrate the effectiveness of transmission power control in reducing energy consumption, none deal with real-time requirements in multi-channel WSNs. Differently, the transmission power configuration proposed in this work is in the multi-channel communication scenario with real-time constraints.

2.3 Received Signal Strength

Several projects have studied received signal strength (RSS) and its utilization in WSNs. Sha et al. [20] establish the model between the RSS and transmission power in a single channel. Demirbas et al. [21] presents a robust and lightweight solution for sybil attack problem based on received signal strength indicator (RSSI) readings of messages in WSNs. However, none of these projects study the relationship between RSS and transmission power in multi-channel WSNs. In this thesis, RSS and PRR models are established for overlapping channels and a transmission power minimization problem based on the models is formulated.

2.4 Real-Time Protocol

Many real-time communication protocols have been proposed for wireless sensor and ad hoc networks. A comprehensive review of real-time communication in WSNs is

presented in [22]. At the MAC layer, Implicit EDF [23] is a collision-free real-time scheduling scheme by exploiting the periodicity of WSN traffic. At higher layers, SPEED [24] achieves desired end-to-end communication delays by enforcing a uniform communication speed throughout the network. However, most of the existing real-time protocols do not take advantage of the capability of multi-channel communications available in today's mote hardware. MCRT, proposed in [6], is the only multi-channel real-time protocol in WSN, which only uses non-overlapping channels. Different from the many previous works, the problem of utilizing overlapping channels is addressed in this thesis for improved real-time performance.

Different from all the aforementioned work that handles real-time guarantees, partially overlapping channels, and energy efficiency in isolation, this work utilizes overlapping channels available on existing sensor mote hardware to achieve more energy-efficient transmission for multi-channel WSNs under real-time constraints.

Chapter 3 Empirical Modeling of Overlapping Channel

Previous work [3] has reported that adjacent overlapping channels have undesired inter-channel interferences. In this chapter, the impacts of overlapping channels on node PRR are first investigated to motivate the work. Based on the motivation and the existing work, an empirical model between RSS and transmission power level for overlapping channels is established. A PRR model to account for the interferences from overlapping channels is derived upon the previous RSS model.

3.1 Case Study for Motivation

In this section, a case study is performed with two pairs of nodes, which compose two one-hop communication links. In the experiment, one pair of motes performs as the transmission pair by using Channel 16. The other pair of motes, acting as the jammer pair, uses Channel 15 to communicate. The transmissions of these two pairs are synchronized. The transmission power of the transmission pair is fixed at power level 15, while the transmission power of the jammer pair increases one level at a time from level 3 to level 31. One hundred packets are transmitted on both pairs at each power level. We calculate the PRR of each pair in this experiment under different transmission power levels of the jammer pair.

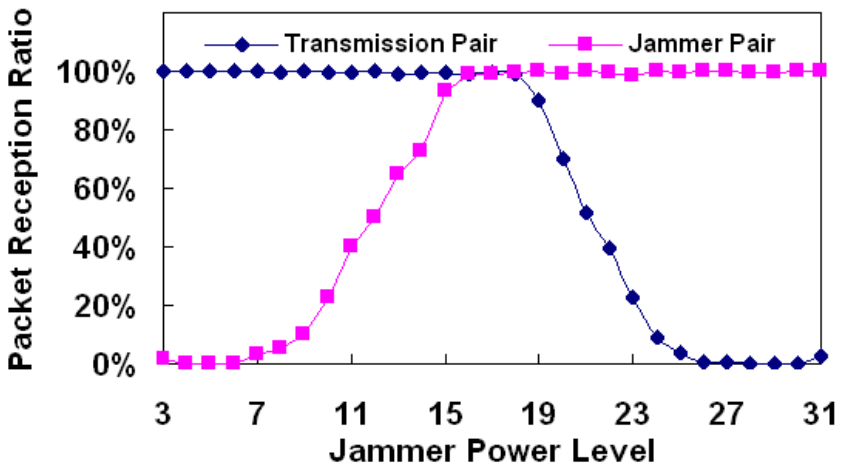

Figure 3.1: Packet Reception Ratio vs. Jammer Power Level

The results are shown in Figure 3.1. From the results we can see that both the two pairs can achieve a good PRR when the jammer pair is using power levels 16 to 18 for transmission. When the jammer is using a lower power level, its communication does not incur much interference to the transmission pair. The transmission pair can reach a high PRR. When the jammer pair is using a higher power level to transmit, it can improve the packet reception ratio of its own communication, but incurs too much interference to the transmission pair, and so hurts the communication quality of the transmission pair. This experiment shows that good quality for concurrent transmissions can be achieved on adjacent overlapping channels if the transmission power is carefully configured.

3.2 Overlapping Channel RSS Model

As discussed in Section 3.1, with careful selection of transmission power, two links working on adjacent channels can both achieve a high PRR. An approximate linear correlation between RSS and transmission power over a single-channel single-hop link is

reported in [20]. In this section, the method proposed in [25] is extended to study the relationship between RSS and transmission power in the scenario where a sender and a receiver are working on adjacent channels. The signal strength detection experiment is conducted on a single link to explore the overlapping channel property.

The experiment uses two Tmote Invent motes. One mote acts as the sender and the other as the RSS sensor. In the experiment, the sender continuously broadcasts packets at a rate of 100 packets per second. The RSS sensor continuously collects the received signal strength by periodically reading the value of the Received Signal Strength Indicator (RSSI) on the mote at a rate of 100 times per second. After every 100 packets, the sender lowers its transmission power by 1 level, starting from level 31 to level 3. The noise is first filtered out by using the noise floor threshold collected before the experiment. Based on the collected values, the average RSS value is calculated. Various combinations of sending and receiving channels are tested in this experiment.

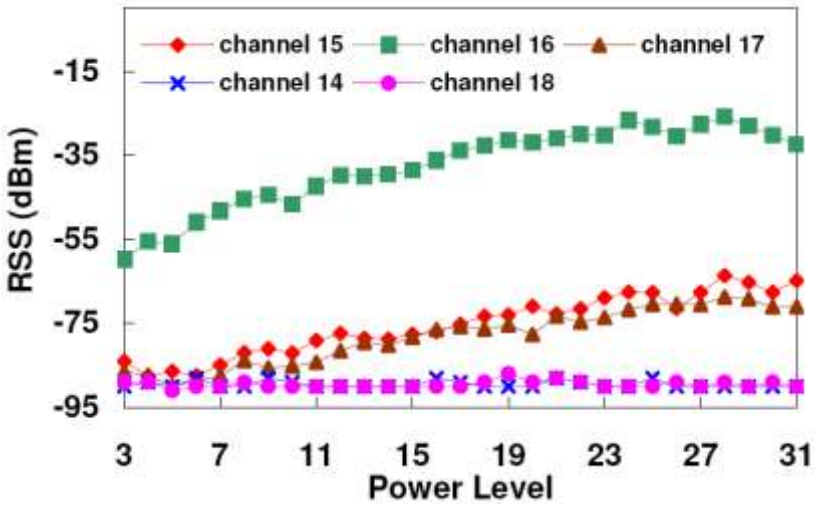

Figure 3.2: RSS vs. Power Level on Different Channels (Sender uses Channel 16)

Figure 3.2 shows the result when the sender is using Channel 16. We can see that when the sender is using Channel 16 for broadcasting, the RSS values sensed on the two adjacent channels, Channel 15 and Channel 17 show highly linear correlation with sender's transmission power. However, no clear RSS reading is sensed on Channel 14 or Channel 18. In addition, the results show an approximate linear increasing trend when the sender and the RSS sensor are using the same channel, Channel 16. Previous work [20] presents the empirical single-channel RSS-Power model as:

$$\mathrm{RSS}(v,u,p_u) = A_{u,v} \times p_u + B_{u,v} \qquad (1)$$

where *v* is the receiving node, *u* is the sending node, and p_u is the transmission power at *u*. *A* and *B* are two parameters of the model, which can be calculated by applying linear curve fitting to the sampled data.

Based on the observation of similar linear pattern when the sender and receiver are using adjacent channels, we can re-establish the empirical RSS-Power model under multi-channel conditions as:

$$RSS(v, u, p_u, c_v, c_u) = A_{u,v,c_v,c_u} \times p_u + B_{u,v,c_v,c_u} \quad (2)$$

where c_u is the transmitting channel for sender u and c_v is the listening channel for receiver v. A similar model is reported in [25]. The model in Equation (2) uses a simplified threshold filter to filter out the noise for faster runtime processing, while a CPM noise filter is used in [25].

Using linear curve fitting to establish this model gives us a fast way to accomplish the model establishment, depending on the number of sampling points needed. One second is required for the signal strength readings for each power level in the model, as explained previously. If 5 power levels are used to build the model, the total time for the model establishment is only 5 seconds. Therefore, the model can be promptly rebuilt at runtime to adapt to environmental or temporal variations of network conditions.

3.3 Packet Reception Ratio Model

Packet reception ratio (PRR) is the probability that a packet can be received successfully. Higher transmission power can provide a higher Signal to Interference and Noise Ratio (SINR) over the link, which leads to a higher PRR. However, with higher transmission power, the communication at the current link could significantly interfere with another link's communication as shown in Section 3.1. In this section, a hardware experiment is conducted to study the relationship between PRR and SINR. With an understanding of this relationship, we can find the appropriate transmission power range to reach a required SINR value for a desired PRR value.

In the experiment, three Tmote Invent motes are used, one as the receiver *C* and the other two as transmitting motes, *A* and *B*. All of the three motes use the same channel. This experiment consists of three rounds. In the first round, only motes *A* and *C* are turned on. Mote A is used to transmit one hundred packets to receiver *C* and we can calculate the average received signal strength of the one hundred packets, denoted as *RSS(A,C)*. In the second round, mote *A* is turned off while mote *B* is turned on to transmit one hundred packets to the receiver. The average received signal strength of *B*, denoted as *RSS(B,C)*, is calculated. In the third round, all the three motes are turned on. Both *A* and *B* transmit one hundred packets to receiver *C*. The transmissions are synchronized. The PRR for *A*'s transmission, denoted as *PRR(A,C)*, can be obtained from this round.

Considering *B*'s transmission as the interference to *A*'s transmission, we can calculate the SINR value for *A*'s transmission as follows:

$$\mathrm{SINR}(\mathrm{A},\mathrm{C})_{\mathrm{dB}} = \mathrm{RSS}(\mathrm{A},\mathrm{C}) - 10\log 10(10^{\frac{\mathrm{RSS}(\mathrm{B},\mathrm{C})}{10}} + 10^{\frac{\mathrm{N}}{10}}) \qquad (3)$$

where N is the noise floor value, which is collected before the experiment. Equation (3) is proposed in [20]. By doing the above three steps and applying the equation, we get a PRR-SINR pair. The experiment is repeated with different distance from B to receiver C and different transmission power levels used by A and B.

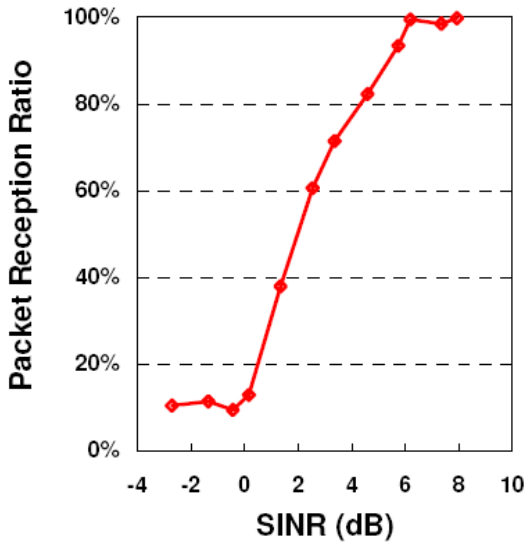

Figure 3.3: PRR vs. SINR Model

Figure 3.3 shows that the PRR-SINR relationship has a 6dB transition range. When the SINR value is greater than 6dB, the PRR is almost 100%. Therefore, in order to achieve a good packet reception ratio, *e.g.*, 90%, we need to choose a transmission power that can provide a strong enough received signal strength leading to an SINR value of more than 6dB.

In order to apply the results to multi-channel networks, we need to extend the PRR-SINR model by incorporating the channel information to it. ($SINR_v$, c_v, PRR_v) is used to denote the PRR-SINR-Channel relationship between node v's packet reception ratio and the corresponding SINR value in channel c_v. With this extended model, we can obtain the required SINR value for a good PRR on a desired channel.

Chapter 4 Minimum Transmission Power Configuration

In this section, the power and channel configuration problem is first formulated. After that, the analysis of the node transmission delay in the network is presented. A heuristic algorithm to calculate the minimum transmission power configuration is then proposed.

4.1 Problem Formulation

We can assume the network has the common many-to-one traffic pattern, which is composed of multiple sources, some relay nodes and one base station. Each source generates a data flow to the base station and all the flows are disjoint. The base station is assumed to be a super node with multiple radios such that it can work on several different frequencies at the same time. The channel allocation in the network is flow-based, which means all nodes in the same flow work on the same channel. The goal is to minimize the total transmission power consumption in the network while the end-to-end delay of every flow is constrained.

Before formulating the minimization problem, the following notation needs to be introduced first:

Table 4.1: Problem Formulation Notations

Notation	*Meaning*
G = (V,E)	A directional graph denoting the network with *V* nodes and *E* edges (links).
f_i	The data flow with the id number *i*
D	The delay constraint for each flow.
p_u	Transmitting power used by node *u*.
c_u	The channel id used by node *u*, which is an integer number
I(v)	The interference node set of node *v*
(u,v)	A communication link in graph, in which *u* is the sending node and *v* is the receiving node

Given the notation above, we can formulate the minimization problem as:

$$\min \sum_{u \in V:(u,v) \in G} p_u \times \frac{1}{PRR(u,v)} \tag{4}$$

Subject to the constraints:

$$1 \le c_u \le n \quad \forall u \in G \tag{5}$$

$$c_{u1} = c_{u2} \quad \text{if } u_1 \in f_j \text{ and } u_2 \in f_j \tag{6}$$

$$\sum_{v \in f_j;(u,v) \in G} \frac{1}{PRR(u,v)} \le D \quad 1 \le j \le m \tag{7}$$

The inverse of *PRR(u,v)* in Equation 4 is the average transmission count required for a packet to be successfully received by node *v* from node *u*. By multiplying p_u and *1/PRR(u,v),* we obtain the transmission power consumption for one packet at node *u*. The objective of Equation 4 is to minimize the total transmission power consumption of all the nodes in the network. Equation 5 is the channel constraint, which confines that each

node can only pick a channel from *n* available channels. Equation 6 confines that all nodes in the same data flow must use the same channel. Equation 7 is the end-to-end delay constraint, which gives the limit of the end-to-end transmission count (including retransmissions at each node) for a packet in each flow. End-to-end transmission count is a commonly used metric to represent end-to-end delay as a higher transmission count leads to a longer end-to-end delay. Note that the minimization problem does not depend on the node duty cycle scheduling, so this work can be integrated with energy-efficient MAC protocols with periodic sleeping for further power savings at the cost of longer communication delays.

4.2 Transmission Delay Analysis

One way to analyze the node transmission delay in a WSN is to use the worst-case scenario, where we can assume that all the links in a neighborhood communicate at the same time, such that the most significant interference and delay are incurred. However, due to the lossy nature of wireless links, real-time communication protocols in WSNs are commonly designed to provide only soft probabilistic real-time guarantees [26][6]. In addition, the traffic in a wireless sensor network is usually event-driven such that the traffic at each source can be assumed to be independently random. The chance for all the links in a neighborhood to transmit at exactly the same time is very small. Therefore, it is more meaningful to analyze the average case for WSNs and the formulation of the optimization problem can be modified as:

$$\min \sum_{u \in V:(u,v) \in G} p_u \times \frac{1}{PRR_{avg}(u,v)} \tag{8}$$

Correspondingly, the end-to-end delay constraint in Equation 7 is modified as:

$$\sum_{v \in f_j;(u,v) \in G} \frac{1}{PRR_{avg}(u,v)} \leq D \quad \forall 1 \leq j \leq m \tag{9}$$

where $PRR_{avg}(u,v)$ is the average packet reception ratio at node v when the generated traffic follows the random distribution.

Note that the probability for more than two nodes to transmit concurrently is small under the random traffic assumption. We can assume that at most two nodes in the same interference range may transmit concurrently. The probability that node w's transmission can interfere with node u's transmission is denoted as $P(u,w)$ and the packet reception ratio at node v of u's transmission under w's interference as $PRR(u,v,w)$. We can use Equation 10 to estimate the average transmission count for node u to successfully transmit a packet to v when u's and w's traffic patterns are independently random.

$$\frac{1}{PRR_{avg}(u,v)} = (1 - \sum_{w \in I(v)} P(u,w)) \frac{1}{PRR(u,v,v)} + (1 - \sum_{w \in I(v)} P(u,w)) \times \frac{1}{PRR(u,v,w)} \tag{10}$$

In Equation 10, $PRR(u,v,v)$ is the packet reception ratio at node v when there is no interference to the sender u's transmission.

Table 4.2: Average PRR Calculation Example

Case	Probability	PRR	1/PRR
No interference at v	25%	100%	1
Interference at v	75%	50%	2

Here we give an example of the calculation. The average transmission count of node *v* given the condition in Table 4.2 is:

$$\frac{1}{\mathrm{PRR}_{\mathrm{avg}}(u,v)} = 25\% \times 1 + 75\% \times 2 \tag{11}$$

Note that *P(u,w)* in Equation 10 is the probability that node *u* and node *w* transmit packets concurrently, under the random traffic pattern assumption. To derive *P(u,w)*, we can first assume that node *u* and node *w* have the same packet rate, 1 packet per *T* seconds, with a packet length *l*. The start time of the transmission at *u* and *w* are denoted as t_u and t_w, respectively. With the assumption that the start time of every packet on each node follows the uniform distribution, we can calculate *P(u,w)* as follows:

$$P(u,w) = \int_0^{l}\int_0^{t_w+l} \frac{1}{T^2}\,dt_u dt_w + \int_l^{T-l}\int_{t_w-l}^{t_w+l} \frac{1}{T^2}\,dt_u dt_w + \int_{T-l}^{T}\int_{t_w-l}^{T} \frac{1}{T^2}\,dt_u dt_w \tag{12}$$

Figure 4.1 illustrates three cases in Equation 12. In the first case, when $t_w \le l$, collision happens under the condition that $t_u \le t_w + l$. In the second case, when $t_w \in (l, T-l]$, collision happens under the condition that $t_u \in (t_w - l, t_w + l]$. In the third case, when $t_w \in (T-l, T]$, collision happens only when $t_u \in (t_w - l, T]$.

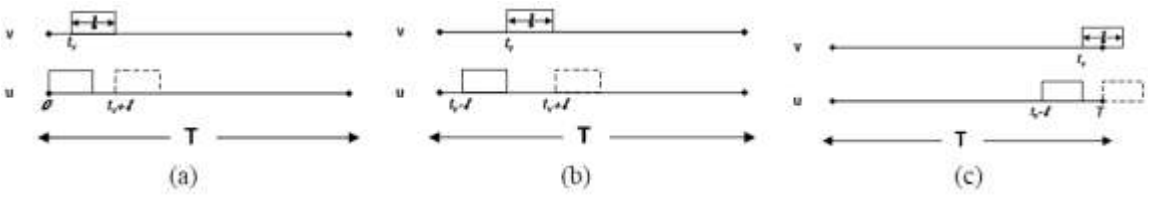

Figure 4.1: Probability of Packet Collision with Independently Random Traffic

By integrating the three cases in Equation 12, the collision probability between two nodes in one period *T* can be calculated as:

$$P(v,u) = \frac{l(2T-l)}{T^2} \tag{13}$$

To verify the average case PRR estimation, an experiment using three motes is conducted, among which two motes act as the senders, *u* and *w*, and the third one as the receiver *v*. First, only *u* is used to transmit packets to *v* and calculate the packet reception ratio, which is the *PRR(u,v,v)* in Equation 10. After that both *u* and *w* are used to transmit packets to the receiver and their transmissions are synchronized. Based on the collected data, we can estimate the packet reception ratio for *u*'s transmission under *w*'s interference, which is the *PRR(u,v,w)* in Equation 10. By substituting Equation 13 into Equation 10, we can calculate the average packet reception ratio, $PRR_{avg}(u,v)$.

The uniform random traffic generators are then implemented on *u* and *w* independently and use both of them to transmit packets to the receiver. The real average packet reception ratio is measured in this round.

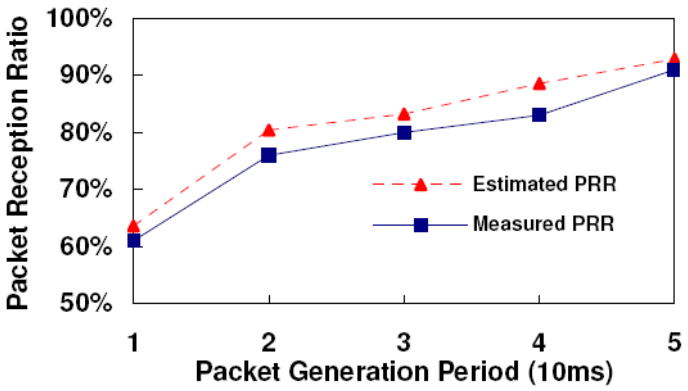

Figure 4.2: Comparison between Estimated Average PRR and Measured Average PRR

The estimated average PRR and the average PRR measured in the real experiment are compared and shown in Figure 4.2. We can see that the estimation is very close to the real experiment result.

Based on the models established in Chapter 3 and a given power level for each node in the network with a channel assignment to the data flows, we can compute the PRR for each receiving node under the interference from another node. By using Equation 10, we can derive the average transmission count for every node and further calculate the end-to-end delay of every flow, as well as the total system power consumption of the network for the given combination of power levels and channels. The optimization objective is to find the combination with the least power consumption while the delay of every data flow is shorter than the given constraint.

4.3 Algorithm Design

The problem formulated in section 4.2 is a complex combinatorial optimization problem with a huge search space. Suppose there are *m* nodes forming *n* flows in the network. The total available number of channels on the equipment is *j*. Each mote can use *k* different power levels to transmit. The combinatorial search space has a size of $j^n k^m$. Therefore, we can use *Simulated Annealing (SA)* [27], a well-known meta-heuristic, to solve this problem. SA is commonly used to find suboptimal solutions when the search space is huge and discrete, which makes SA well suited for the proposed optimization problem because all possible configuration states are discrete, as the selection of channels and power levels are discrete numbers.

Simulated Annealing is a probabilistic method for global optimization problems. It transposes the physical process of the annealing of metal, in which the temperature of the metal is gradually decreased, to the solution search of the optimization problem. In each step, the algorithm considers some neighbor states of the current state, and chooses a valid neighbor state for the next state according to a probabilistic function established on the optimization goal. Two major parts of *SA* are the neighbor state generation and the transition probability. The neighbor state generation scheme requires that every two adjacent states have a short distance. The transition probability is to decide whether the system should go to the next state, *i.e.*, the neighbor state generated in the neighbor generation part.

Algorithm 1 Simulated Annealing for Power Consumption Minimization

Denote delay constraint as D, the stop flag as T_{end}, and the starting flag as T_{ini}. The initial channel configuration is C_{ini}. P_{ini} is the initial power consumption. ρ is the factor of temperature decreasing.

$T \Leftarrow T_{ini}$. $C \Leftarrow C_{ini}$.$n \Leftarrow 0$. $P \Leftarrow P_{ini}$

while $T \geq T_{end}$ **do**

  Find neighbor configuration C_{temp}. Calculate power consumption P_{temp} and $delay_i$ for each data flow i

  if $\forall delay_i \leq D$ **then**

    $\Delta P \Leftarrow P_{temp} - P$;

  else

    $\Delta P \Leftarrow P_{temp} + Penalty - P$;

  end if

  if $\Delta P \leq 0$ **then**

    $C \Leftarrow C_{temp}$; $P \Leftarrow P_{temp}$

  else

    if $e^{-\frac{\Delta P}{T}} \geq random()$ **then**

      $C \Leftarrow C_{temp}$; $P \Leftarrow P_{temp}$

    end if

  end if

  $n \Leftarrow n + 1, T \Leftarrow \rho^n T_{ini}$

end while

Figure 4.3: Algorithm of Simulated Annealing for Minimum Power Configuration

In the formulated problem, the objective is to minimize the total transmission power consumption for the network under an end-to-end flow delay constraint. The configuration space consists of all the channel assignment and power configuration combinations.

Based on the given channel and power configuration, the system will proceed to the next configuration by conducting an elementary modification. The elementary modification is defined as a channel change on one of the flows or a power level change on one of the nodes. The pseudo code of the algorithm is given by Algorithm 1 in Figure 4.3.

The algorithm starts with an initial "temperature" T_{ini} and an initial configuration C_{ini} with initial power consumption P_{ini}. It then looks for a neighbor configuration as the next configuration state, C_{temp}. After a neighbor is found, the algorithm first checks if the delay $Delay_i$ of every data flow under the neighbor configuration meets the delay

constraint D. If the constraint is met, the algorithm calculates the power consumption difference, ΔP, at the neighbor state and the current state. However, if the constraint is violated, the algorithm adds a *Penalty* to ΔP. The *Penalty* is a parameter that needs to be tuned for the experiment in order to get a good solution. It helps the algorithm to avoid being trapped at a local minimum. The algorithm then checks if the power consumption is reduced. If the power consumption is reduced, the neighbor configuration is accepted. However, if the neighbor configuration causes an increased ΔP for power consumption, the algorithm calculates a probability by the exponential expression $e^{-\frac{\Delta P}{T}}$ and accepts the neighbor configuration based on this probability. After each iteration, the ``temperature'' is decreased by a factor of ρ. The algorithm ends when the "temperature" is smaller than the threshold T_{end}.

Chapter 5 Empirical Results

The evaluation results of the configuration algorithm on the hardware testbed are presented in this chapter.

5.1 Testbed Setup and Baselines

The testbed used in the experiment consists of 25 Tmote Invent motes. Three different topologies used for the experiment are shown in Figure 5.1. Node 13, as the base station, consists of 5 real motes in the experiment, which emulates a super node with 5 radios. Independent uniform random traffic generators are implemented on each source node.

We first need to collect background noise and the RSS measurement at each node to establish the RSS-Power model from Section 3. A base station is used to measure the background noise. The base station stays in a channel for a while and measures the average RSS for the background noise of each channel.

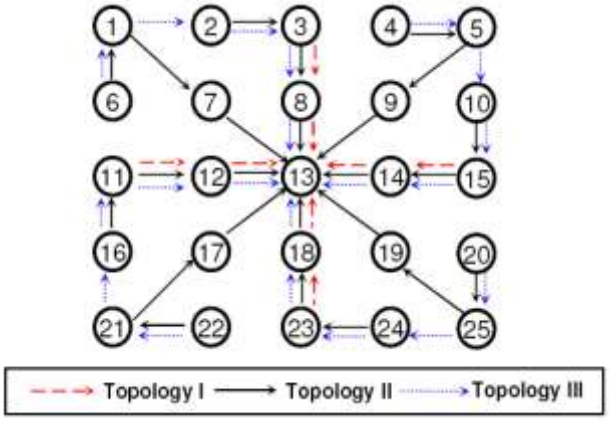

Figure 5.1: Topologies Used in Experiments

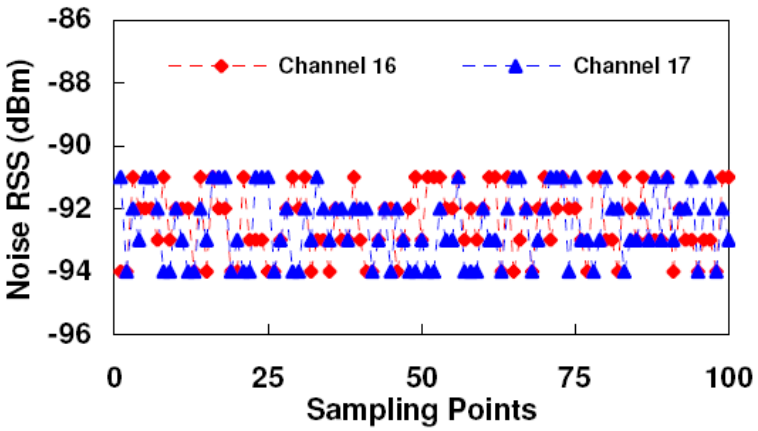

Figure 5.2: Background noise measurement

Figure 5.2 shows the result of the background noise of channels 16 and 17 in the experimental environment. We can see that all the background noise is lower than -90dBm. Therefore, we take -90dBm as the noise strength of the experiment environment.

In the RSS measurement phase, every mote in the network takes turn to act as the sender and broadcasts packets using different power levels on different channels. While the sender is sending packets at a certain power level on a fixed channel *c*, all other nodes acting as listeners iterate through channel *c-1*, *c* and *c+1*, and record the received signal strength on each channel. The reason that only three channels are chosen to listen is because only the same channel and adjacent channels show the approximate linear PRR-Power pattern, as discussed in Chapter 3. In the experiments, 5 discrete power levels are used: 3, 10, 17, 24 and 31, as the transmission power for the model establishment. This helps us to reduce the solution search space to speed up the experiments. After all the RSS measurements are collected, the data is imported to the Simulated Annealing optimization program we implemented in Matlab to compute the channel and power configuration.

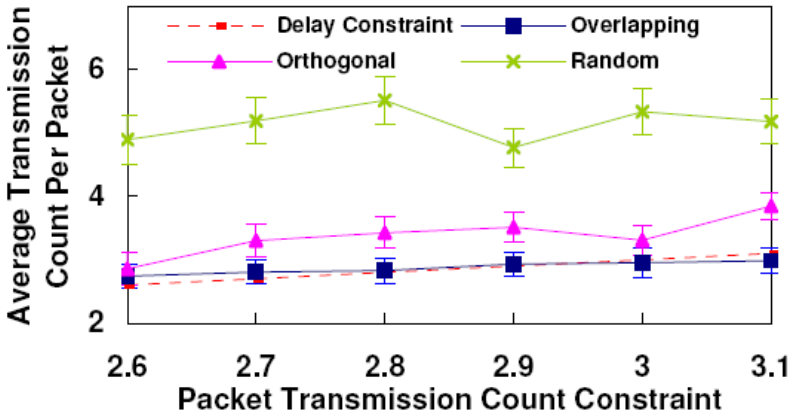

Figure 5.3: Delay under Different End-to-end Transmission Delay Constraints

The following two baselines are chosen for comparison. The first baseline, called *Orthogonal*, uses only orthogonal channels for channel assignment and computes the power configuration by Simulated Annealing Algorithm. The second baseline, called *Random*, also uses Simulated Annealing to find the desired power level for each node, but randomly assigns overlapping channels to flows.

5.2 Different Delay Constraints

The proposed scheme is first evaluated under different transmission count constraints. In this experiment, Topology I in Figure 5.1 with nine motes is used, forming 4 flows. Three channels, 16, 17 and 18, are used. Channel 16 and 18 are orthogonal channels while channel 17 overlaps with channels 16 and 18. Figure 5.3 shows the average end-to-end delay under different constraints. The overlapping scheme achieves a smaller average end-to-end transmission count than the two baseline schemes. In addition, the delay of the overlapping scheme is closest to the constraints. With the constraint becoming loose, all the schemes yield high end-to-end transmission counts. This

indicates that the end-to-end delay in the network is adaptive to the change of the delay constraint. The superior performance of the overlapping scheme demonstrates that taking advantage of overlapping channels with carefully selected power and channel configurations can improve the real-time performance of the network.

Figure 5.4 shows the transmission power consumption per packet for different constraints. The overlapping scheme consumes the least transmission power among all the schemes. When the constraint is greater than 2.8, the performance of *Orthogonal* is close to that of the overlapping scheme. However, when the constraint is tight, *Orthogonal* performs significantly worse than the overlapping scheme. All the three schemes show decreasing trends for power consumption while the end-to-end transmission constraint is becoming looser. This is because when the constraint is loose, we have a larger search space for the SA algorithm, resulting in a better power configuration. The experiments demonstrate that the overlapping scheme saves more power by taking advantage of the overlapping channel resources.

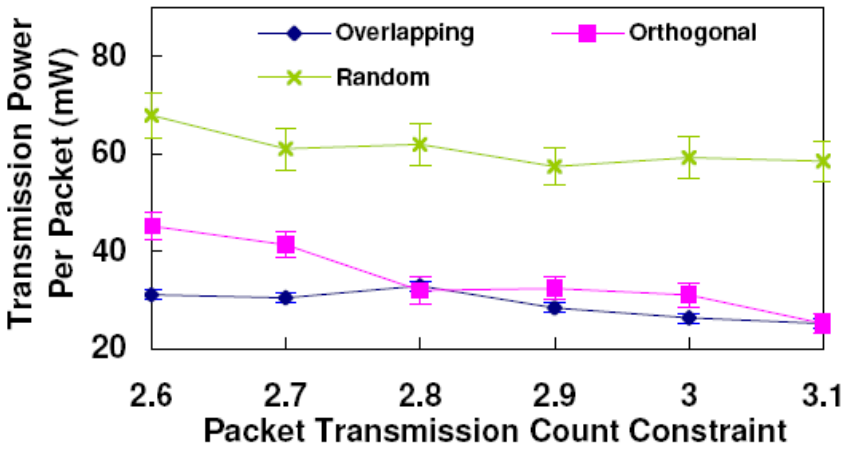

Figure 5.4: Power Consumption under Different End-to-end Transmission Delay Constraints

5.3 Different Packet Rates

In this section, the impact of different packet rates is evaluated. The topology used in this experiment is Topology I in Figure 5.1. The end-to-end transmission count constraint is set to 4 for all the experiments in this subsection.

Figure 5.5 shows that the overlapping scheme has the smallest end-to-end transmission count under different inter-packet intervals. When the inter-packet time increases from 50ms to 100ms at a step of 10ms, the average transmission count per packet decreases for all the schemes. This demonstrates that a higher packet rate can cause a higher degree of packet collision and thus an increased retransmission count for each packet. However, with the advantage of overlapping channels, the end-to-end delay can be reduced at all different packet rates.

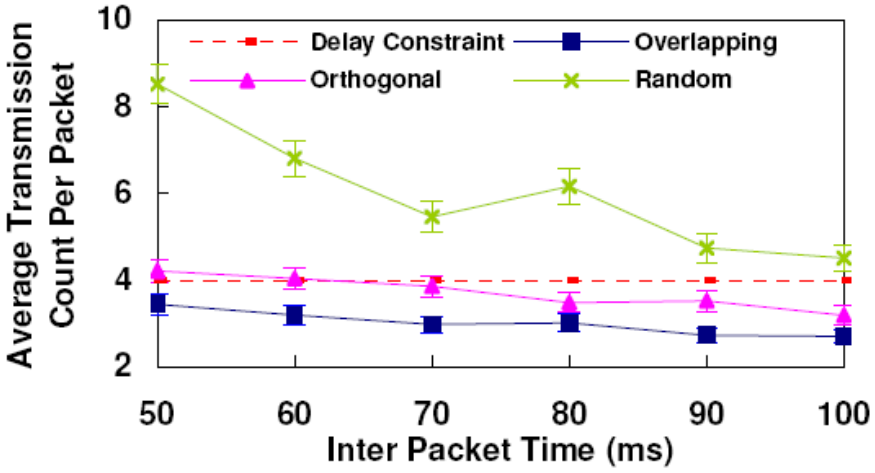

Figure 5.5: Delay under Different Packet Rates

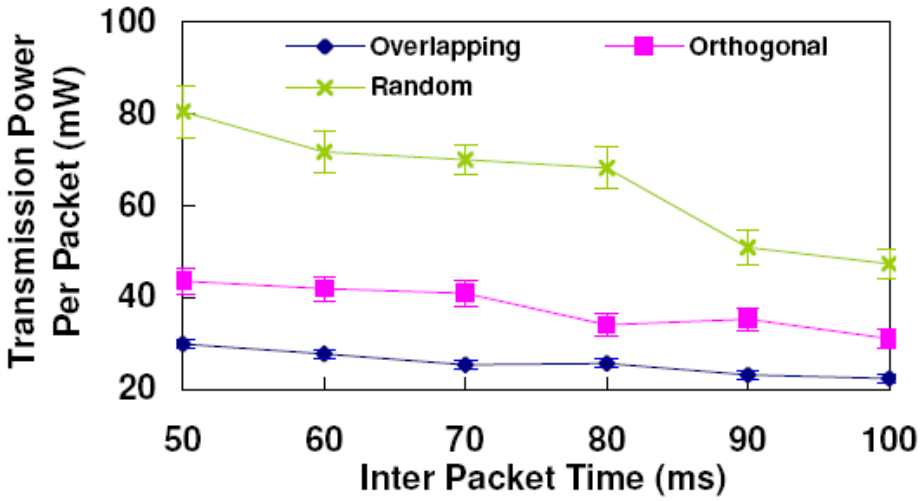

Figure 5.6: Power Consumption under Different Packet Rates

Figure 5.6 plots the transmission power consumption under different packet rates. It can be observed that a lower packet rate leads to reduced power consumption. This is consistent with the trend of average transmission count in Figure 5.5, as decreasing packet transmission count can reduce power consumption. The overlapping scheme achieves the most power savings among all the three schemes, indicating that appropriate utilization of overlapping channels with careful power configuration can lead to significant power savings.

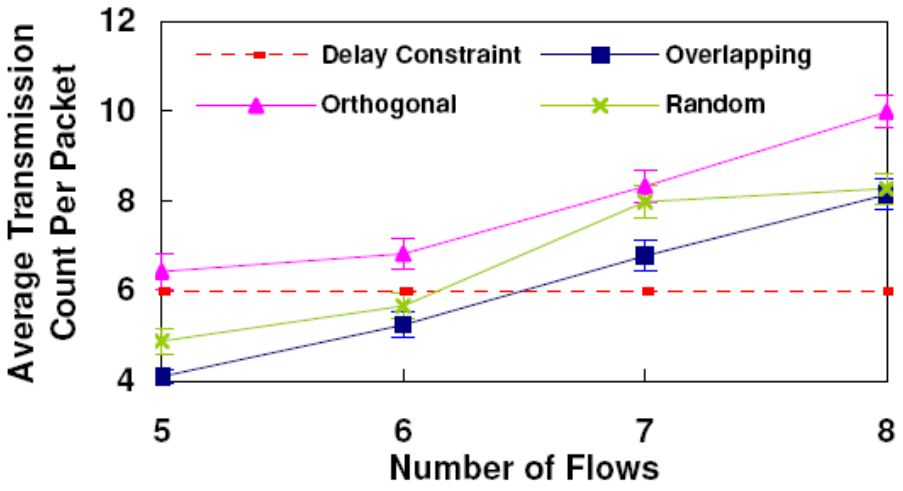

Figure 5.7: Delay under Different Numbers of Data Flows

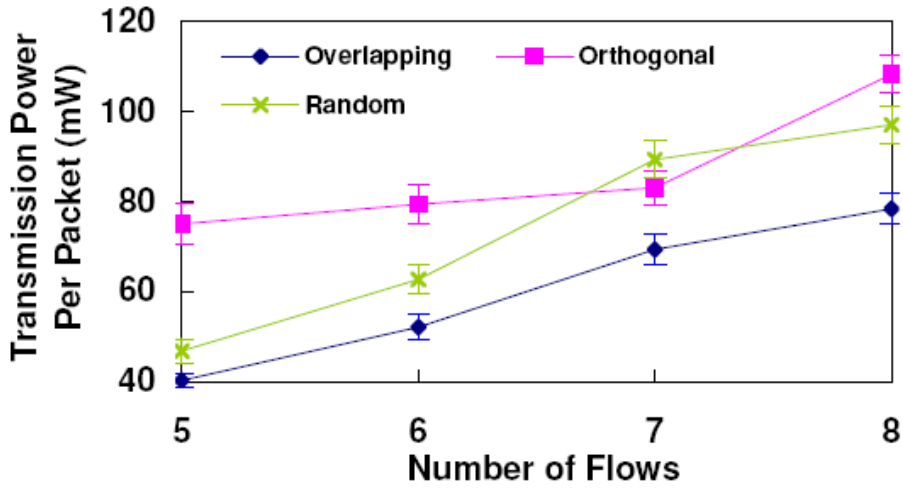

Figure 5.8: Power Consumption under Different Numbers of Data Flows

5.4 Different Flow Numbers

Figures 5.7 and 5.8 show the performance of the network with different numbers of data flows. It is important to evaluate the performance of the network under different numbers of flows because multiple flows may need to share channels when the number of flows increases. In these experiments, Topology II in Figure 5.1 is used, where 25 motes are organized as a 5 by 5 grid. The base station is placed in the center, similar to the previous two experiments. Each data flow has three hops and the number of data flows in the network is increased gradually from 5 to 8. Five overlapping channels are used, from channel 16 to channel 20, where 3 channels are orthogonal.

Figure 5.7 shows that the average transmission count per packet increases when the number of data flows increases. This is because more data flows bring more interference into the network and more flows are sharing the same channels for data transmissions. The same trend can be observed for power consumption. Among all three schemes, the overlapping scheme performs best for both the average transmission count and average power consumption. The reason is that the overlapping scheme considers the impacts from the adjacent channels and configures transmission power to reduce the interferences with adjacent channels. Note that *Orthogonal* performs the worst because a greater number of flows need to share channels when there are only 3 *orthogonal* channels available. The increased channel sharing leads to a higher degree of channel competition and intra-channel interferences, and thus more packet retransmissions.

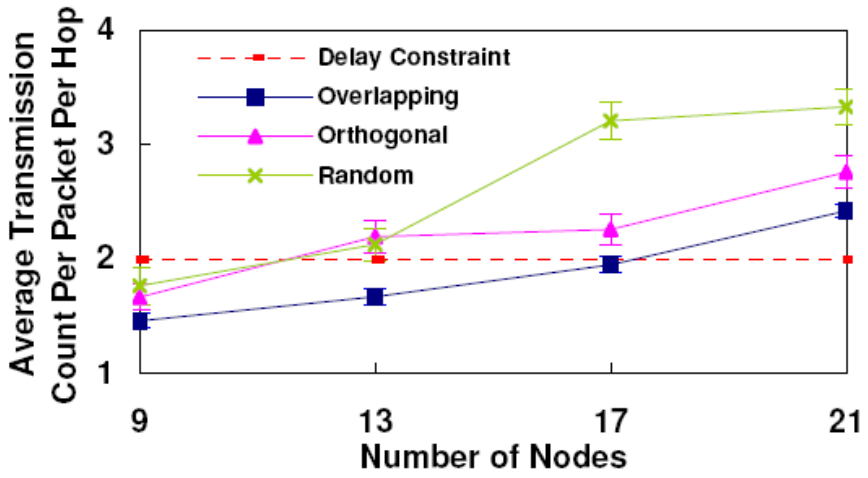

Figure 5.9: Delay under Different Network Sizes

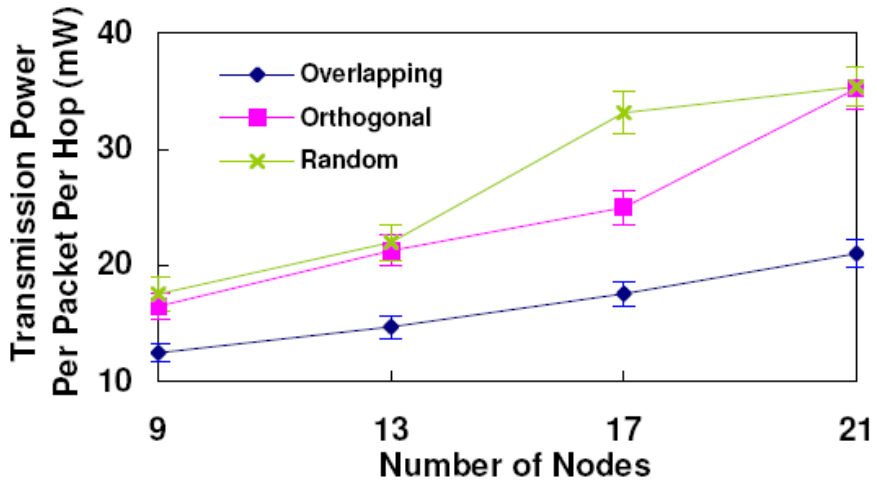

Figure 5.10: Power Consumption under Different Network Sizes

5.5 Different Network Sizes

In this set of experiments, the network size is varied by adding more hops to each flow. Topology III in Figure 5.1 is used where 4 flows are organized in the network. Three channels are used, two of which are orthogonal channels. The size of the network is increased from 9 motes to 21 motes, by adding one more mote to each flow at a time. The performances of the three schemes are evaluated in terms of average transmission count and transmission power.

From Figures 5.9 and 5.10, we can see that when the network size increases, both the average transmission count and power consumption increase. The reason is that when there are more nodes in each data flow, the intra-flow interference is increased due to a higher degree of channel competition. In addition, the inter-flow interference also increases because more nodes are competing for the channel shared by flows. Among all the three schemes, the overlapping scheme yields the lowest power consumption and transmission counts. This experiment demonstrates that even though having more transmitting nodes in a network may lead to increased interferences and degraded real-time performance, utilizing overlapping channels with careful power configuration can alleviate the impacts.

Chapter 6 Conclusion

Multi-channel communications can improve the network throughput and end-to-end real-time guarantees in a WSN with reduced power consumption. However, recent studies suggest using only orthogonal channels because adjacent overlapping channels may have undesired inter-channel interferences. As the number of orthogonal channels available on today's mote hardware is small, using only orthogonal channels has limited the further improvement of real-time performance and power optimization, when the number of data flows is large in a network.

In this work, empirical studies have been conducted to investigate the interferences among overlapping channels. The results show that overlapping channels can also be utilized for improved real-time performance if the transmission power is carefully configured. In order to minimize the overall power consumption of a network with multiple data flows under end-to-end delay constraints, a constrained optimization problem is formulated to configure the transmission power level for every node and assign overlapping channels to different data flows. Since the optimization problem has an exponential computational complexity, a heuristic algorithm designed based on Simulated Annealing is then proposed to find a suboptimal solution. The extensive empirical results on a 25-mote testbed demonstrate that the proposed algorithm reduces both the end-to-end communication delay and overall transmission power consumption, compared with two baselines: a scheme using only orthogonal channels and a scheme using simple policy to assign overlapping channels.

List of References

List of References

[1] "Cc2420 2.4 ghz ieee 802.15.4 / zigbee-ready rf transceiver." [Online]. Available: http://www.chipcon.com.

[2] P. Gupta and P. R. Kumar, "*The capacity of wireless networks*," IEEE Transactions on on Information Theory, vol. 46, no. 2, 2000.

[3] Y. Wu, J. Stankovic, T. He, and S. Lin, "*Realistic and efficient multichannel communications in dense sensor networks,*" in INFOCOM, 2008.

[4] J. Zhang, G. Zhou, C. Huang, S. H. Son, and J. A. Stankovic, "*TMMAC: An energy efficient multi-channel mac protocol for ad hoc networks*," in ICC, 2007.

[5] G. Zhou, C. Huang, T. Yan, T. He, J. A. Stankovic, and T. F. Abdelzaher, "*MMSN: Multi-frequency media access control for wireless sensor networks,*" in INFOCOM, April 2006.

[6] X. Wang, X. Wang, G. Xing, and F. Xing, "Flow-based real-time communication in multi-channel wireless sensor networks," in EWSN, 2009.

[7] H. Liu, H. Yu, X. Liu, C.-N. Chuah, and P. Mohapatra, "*Scheduling multiple partially overlapped channels in wireless mesh networks,*" in ICC, 2007.

[8] Z. Feng and Y. Yang, "*How much improvement can we get from partially overlapped channels?*" in WCNC, 2008.

[9] A. H. M. Rad and V. W. Wong, "*Partially overlapped channel assignment for multi-channel wireless mesh networks,*" in ICC, 2007.

[10] P. Santi, "*Topology control in wireless ad hoc and sensor networks,*" Istituto di Informatica e Telematica, Pisa - Italy, Tech. Rep. IIT-TR-04, 2003.

[11] R. Ramanathan and R. Hain, "*Topology control of multihop wireless networks using transmit power adjustment,*" in INFOCOM, 2000.

[12] L. Li, J. Y. Halpern, P. Bahl, Y.-M.Wang, and R.Wattenhofer, "*Analysis of a cone-based distributed topology control algorithm for wireless multi-hop networks*," in PODC, 2001.

[13] N. Li, J. C. Hou, and L. Sha, "*Design and analysis of an mst-based topology control algorithm,*" in INFOCOM, 2003.

[14] D. Son, B. Krishnamachari, and J. Heidemann, "*Experimental study of the effects of transmission power control and blacklisting in wireless sensor networks,*" in SECON, 2004.

[15] S. Singh, M. Woo, and C. S. Raghavendra, "*Power-aware routing in mobile ad hoc networks,*" in MobiCom, 1998.

[16] Q. Li, J. Aslam, and D. Rus, "*Online power-aware routing in wireless ad-hoc networks,*" in MobiCom, 2001.

[17] J.-H. Chang and L. Tassiulas, "*Energy conserving routing in wireless ad-hoc networks,*" in INFOCOM, 2000.

[18] A. Sankar and Z. Liu, "*Maximum lifetime routing in wireless ad-hoc networks,*" in INFOCOM, 2004.

[19] S. Doshi, S. Bhandare, and T. X. Brown, "*An on-demand minimum energy routing protocol for a wireless ad hoc network,*" SIGMOBILEMob. Comput. Commun. Rev., vol. 6, no. 3, pp. 50–66, 2002.

[20] M. Sha, G. Xing, G. Zhou, S. Liu, and X. Wang, "*C-mac: Model-driven concurrent medium access control for wireless sensor networks,*" in INFOCOM, 2008.

[21] M. Demirbas and Y. Song, "*An rssi-based scheme for sybil attack detection in wireless sensor networks,*" in WoWMoM, 2006.

[22] J. A. Stankovic, T. Abdelzaher, C. Lu, L. Sha, and J. Hou, "*Real-time communication and coordination in embedded sensor networks,*" Proceedings of the IEEE, vol. 91, no. 7, 2003.

[23] M. Caccamo, L. Y. Zhang, and L. Sha, "*An implicit prioritized access protocol for wireless sensor networks,*" in RTSS, 2002.

[24] T. He, J. Stankovic, C. Lu, and T. Abdelzaher, "*SPEED: A stateless protocol for real-time communication in sensor networks,*" in ICDCS, 2003.

[25] G. Xing, M. Sha, J. Huang, G. Zhou, X. Wang, and S. Liu, "*Multi-channel interference measurement and modeling in low-power wireless networks,*" Michigan State University, Tech. Rep. MSU-CSE-09-20, 2009.

[26] O. Chipara, Z. He, G. Xing, Q. Chen, X. Wang, C. Lu, J. Stankovic, and T. Abdelzaher, "*Real-time power-aware routing in sensor networks,*" in IWQoS, 2006.

[27] S. Kirkpatrick, C. D. G. Jr., and M. P. Vecchi, "*Optimization by simulated annealing,*" Science, vol. 220, no. 4598, pp. 671–680. 13

Vita

Xiaodong Wang is the candidate of Master of Science in the Department of Electrical Engineering and Computer Science at the University of Tennessee, Knoxville. He is currently working as a Graduate Assistant under the supervision of Dr. Xiaorui Wang in the PACS Lab. He is the recipient of the first Min Kao Scholarships of Electrical and Computer Engineering in the EECS department. Xiaodong Wang received his B.S. degree in Electrical Engineering from Shanghai Jiaotong University, China, in 2006. In 2007, he worked at PDF Solutions Inc. as a data analyst.